



Pergamon

Tetrahedron 56 (2000) 7011–7018

TETRAHEDRON

# Construction of Peptides That Undergo Structural Transition from $\alpha$ -Helix to $\beta$ -Sheet and Amyloid Fibril Formation by the Introduction of N-Terminal Hydrophobic Amino Acids

Yuta Takahashi,<sup>a,†</sup> Taro Yamashita,<sup>a</sup> Akihiko Ueno<sup>a</sup> and Hisakazu Mihara<sup>a,b,\*</sup>

<sup>a</sup>Graduate School of Bioscience and Biotechnology, Department of Bioengineering, Tokyo Institute of Technology, Nagatsuta, Midori-ku, Yokohama 226-8501, Japan

<sup>b</sup>Form and Function, PRESTO, Japan Science and Technology Corporation, Yokohama 226-8501, Japan

Received 10 January 2000; revised 17 February 2000; accepted 19 February 2000

**Abstract**—Recent studies on amyloid disease-related proteins such as  $\beta$ -amyloid and prion have pointed out that conformational alternation and subsequent aggregation to form amyloid fibrils play a key role in such fatal diseases. Here, design and synthesis of peptides undergoing a structural transition from  $\alpha$ -helix to  $\beta$ -sheet and self-assembly into amyloid fibrils are described. A dimeric peptide was designed to form a coiled-coil  $\alpha$ -helix structure and the N-terminus was modified with various kinds of standard hydrophobic amino acids. The self-initiated structural transition to  $\beta$ -sheet was induced by appropriate hydrophobic amino acids attached to the N-termini of the peptides. Moreover, the peptides in  $\beta$ -sheet self-assembled into the amyloid with a well-organized fibrillar structure. Simplified model peptides like those presented here will lead to a better understanding of the process by which conformational alternation and aggregation of proteins occur, as well as to developing novel nanoscale materials. © 2000 Elsevier Science Ltd. All rights reserved.

## Introduction

Capability of both intra- and intermolecular self-assembly of polypeptide chains is one of the most important features of proteins, which generates a well-defined three dimensional structure depending on their amino acid sequences. However, a folding of polypeptide chain into an undesired structure and resultant aggregation could occur due to several reasons.<sup>1–4</sup> Recently, such a misfolding of proteins has attracted much attention, since it is closely related to a number of fatal diseases.<sup>1–7</sup> Amyloid is a fibrillar aggregate of misfolded proteins, which has been proposed to be a causative agent of amyloid diseases such as Alzheimer's and prion diseases.<sup>7–14</sup> Amyloid fibril formation is called misassembly, since it is an undesired state and would cause fatal diseases. On the other hand, it is also considered that the amyloid fibril is a self-assemblage with a highly ordered quaternary structure.<sup>7</sup> It has been proposed that  $\beta$ -strands align perpendicularly to the fiber axis with regular strand spacings.<sup>7</sup>

The pathway of protein misfolding and subsequent fibril formation involves a conformational transition, for example, from  $\alpha$ -helix to  $\beta$ -sheet structure. This transition is especially apparent in the conversion of prion proteins from normal to abnormal isoform without any chemical modification.<sup>12–14</sup> The cellular form of the prion protein (PrP<sup>C</sup>) is rich in an  $\alpha$ -helix structure and highly water-soluble, but the scrapie isoform (PrP<sup>Sc</sup>) forms amyloid fibrils with a higher  $\beta$ -sheet content. Similarly,  $\beta$ -amyloid peptide, which is a major component of the amyloid plaques deposited in the brains of Alzheimer's disease patients, has an  $\alpha$ -helical propensity in some environments.<sup>8–11</sup> It is becoming increasingly important to study the nature of the proteins in order to understand such critical diseases. Furthermore, medium-controlled amyloid fibril formation of proteins which are not associated with any amyloid disease has been reported.<sup>15,16</sup> Although a variety of proteins are known to form amyloid fibrils, no obvious sequence or structural similarity for these proteins has been suggested. Thus, a simplified model peptide would lead to a better understanding of the process by which misfolding and fibril formation of proteins occur.

Peptides based on the de novo design have provided useful information for constructing and manipulating peptide conformation, and elucidating complex folding mechanisms.<sup>17–19</sup> Design of peptides to adopt a  $\beta$ -sheet folding<sup>18,19</sup> and a fibrillar structure like amyloid fibrils<sup>20–24</sup> has been a current interest as well as creation of native-like globular de

**Keywords:** peptides and polypeptides; self-assembly; amyloid fibril; structural transition;  $\alpha$ -helix;  $\beta$ -sheet; molecular design; conformation; aggregation.

\* Corresponding author. Graduate School of Bioscience and Biotechnology, Department of Bioengineering, Tokyo Institute of Technology, Nagatsuta, Midori-ku, Yokohama 226-8501, Japan. Tel.: +81-45-924-5756; fax: +81-45-924-5833; e-mail: hmihara@bio.titech.ac.jp

† Research fellow of the Japan Society for the Promotion of Science

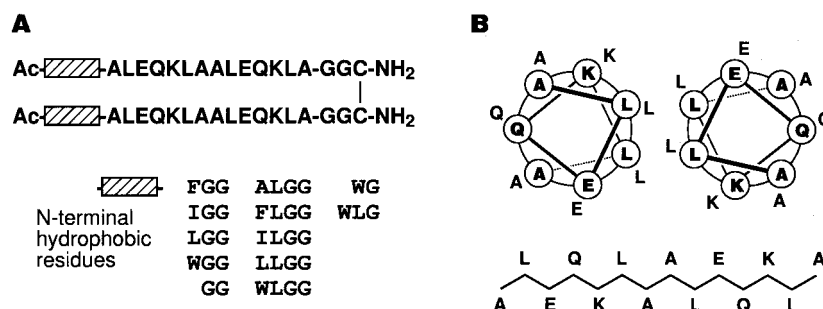


**Figure 1.** (A) Primary structure of the peptides with hydrophobic amino acids at N-termini. (B) A helix wheel drawing as a coiled-coil form and a  $\beta$ -strand drawing of the core 14-peptide. Abbreviations for amino acids are: A, alanine; C, cysteine; E, glutamic acid; F, phenylalanine; G, glycine; I, isoleucine; K, lysine; L, leucine; Q, glutamine; W, tryptophan.

novo proteins.<sup>17</sup> Designing sequences of peptides to allow conformational interconversions, e.g. helix-sheet switching, has been widely attempted,<sup>25–32</sup> which includes sequence manipulation of natural proteins<sup>25–27</sup> and de novo sequence design.<sup>28–32</sup> Furthermore, similar  $\alpha$ -to- $\beta$  structural transition has been proposed in a correct-folding pathway with a non-hierarchical mechanism.<sup>33</sup> These studies suggest that both overall and local conformations of proteins and their conversion are critically determined by long-range interactions including both intra- and intermolecular interactions between secondary structures as well as by short-range interactions between nearby amino acid residues.

Recently, we have reported the design of peptides that undergo self-initiated  $\alpha$ -to- $\beta$  structural transition and fibril formation, which are caused by the exposure of a hydrophobic domain attached to the N-terminus.<sup>34,35</sup> The first success of this approach for designing  $\alpha$ -to- $\beta$  transitional peptides was accomplished by using 1-adamantanecarbonyl (Ad-) group as the N-terminal hydrophobic domain of the  $2\alpha$ -helix peptide.<sup>34</sup> In an aqueous solution, the Ad-linked  $2\alpha$ -peptide underwent an  $\alpha$ -to- $\beta$  transition and amyloid fibril formation in an autocatalytic manner. To explore the effect of the hydrophobic domain, we synthesized the peptides with a variety of aliphatic acyl chains at the N-termini and examined the conformational properties.<sup>35</sup> It became clear that acyl chains of particular length caused the peptides to undergo an  $\alpha$ -to- $\beta$  transition, and there was an optimum length (hydrophobicity), such as the octanoyl (C8-) group, for the transition. The peptides that we previously designed included non-amino acid moieties such as Ad-group or acyl chains.<sup>34,35</sup> We have been interested in whether these N-terminal non-amino acid moieties are replaceable by standard hydrophobic amino acids. Design of peptides composed of only standard amino acids retaining the ability of undergoing the  $\alpha$ -to- $\beta$  structural transition and amyloid fibril formation has been desired, since such peptides would provide further insight into phenomena exhibited by naturally occurring amyloidogenic proteins than peptides with non-amino acid moieties. We thereby report here design and synthesis of a variety of peptides with hydrophobic amino acids at the N-termini, and comparison of the ability of undergoing the  $\alpha$ -to- $\beta$  structural transition and amyloid fibril formation. It has been shown that particular hydrophobic amino acids

attached to the N-termini are able to initiate the  $\alpha$ -to- $\beta$  structural transition and amyloid fibril formation.

## Results and Discussion

### Design of peptides

Peptides undergoing  $\alpha$ -to- $\beta$  structural transitions and amyloid fibrillogenesis were designed as previously described.<sup>34,35</sup> A homodimeric peptide composed of two amphiphilic  $\alpha$ -helices was designed (Fig. 1). The  $2\alpha$ -helix part was constructed from amino acid sequences of coiled-coil proteins,<sup>36</sup> which had heptad repeats (abcdefg)<sub>n</sub> with hydrophobic residues at the a and d positions (Fig. 1B). However, when the peptide sequence was drawn as a  $\beta$ -strand model, the peptide could take a kind of amphiphilic  $\beta$ -strand structure, in which hydrophobic leucine residues and hydrophilic glutamic acid and lysine residues were separated on different faces (Fig. 1B). It has been suggested that one cause of protein misfolding and aggregation is thought to be the exposure of the hydrophobic region of proteins in a relatively unstable states to an aqueous environment, which is caused by an environmental change or an unfavorable mutation. Based on this, in the previous models,<sup>34,35</sup> hydrophobic Ad-group or aliphatic acyl chains were attached to the N-termini as an exposed hydrophobic domain which facilitated the peptide aggregation. In this study, instead of the Ad-group or acyl chains, one or two hydrophobic amino acids (alanine, isoleucine, leucine, phenylalanine and tryptophan) were attached to the N-termini of the peptide as shown in Fig. 1A. The two segments were linked to form a parallel homodimer by the disulfide bond between cysteine residues at the C-termini. Two glycine residues were employed for spacers to connect the N-terminal hydrophobic amino acids or the C-terminal cysteine to the core 14-residue peptide. Peptides with single glycine as the N-terminal spacer were also examined. In the previous models, single  $\beta$ -alanine residue was employed for both N-terminal and C-terminal spacers.<sup>34,35</sup>

All peptides were synthesized by the solid-phase method using 9-fluorenylmethyloxycarbonyl (Fmoc) chemistry.<sup>37</sup> The fully deprotected peptides were oxidized to form the intermolecular disulfide bond. The peptides were purified by reversed-phase HPLC, and identified by matrix assisted

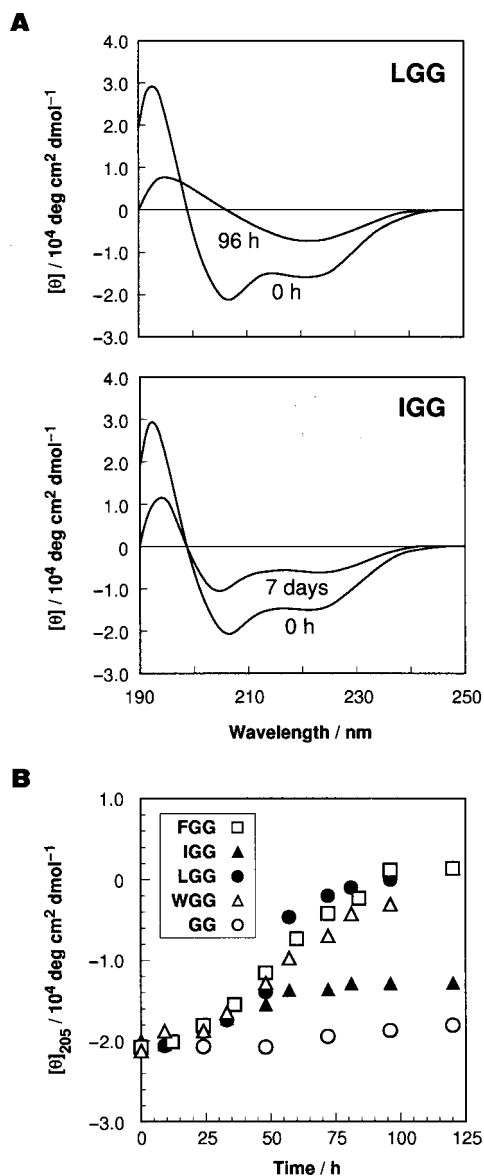


**Figure 2.** CD studies of the peptides with one hydrophobic residue at N-termini. (A) Time-dependent CD spectral changes of LGG and IGG. (B) Time courses of structural transitions of the peptides monitored by the molar ellipticity at 205 nm. [Peptide]=12–14  $\mu\text{M}$  in 20 mM Tris-HCl buffer (pH 7.4)/2.5% TFE at 25°C.

laser desorption ionization time-of-flight mass spectrometry (MALDI-TOFMS) and amino acid analysis.

### Structural transition of the peptides from $\alpha$ -helix to $\beta$ -sheet

The conformational changes of the peptides with one hydrophobic residue at the N-termini (FGG, IGG, LGG and WGG) were examined by circular dichroism (CD) spectroscopy (Fig. 2). All peptides showed CD spectra typical for an  $\alpha$ -helix structure shortly after dilution in 20 mM Tris-

HCl buffer (pH 7.4) from the trifluoroethanol (TFE) solution (final peptide concentration, 12–14  $\mu\text{M}$ ; TFE content, 2.5%).<sup>11</sup> The CD measurements were carried out after various incubation periods. Although the peptides with the hydrophobic amino acids showed gradual changes in their spectra, the conformational changing properties were different depending on the amino acids attached to the N-termini. FGG, LGG and WGG changed their spectra from those typical for  $\alpha$ -helix to  $\beta$ -sheet after 4 days (Fig. 2A), and the time courses of the structural transitions detected by the ellipticity at 205 nm were not significantly different (Fig. 2B). Although the peptides in the  $\beta$ -sheet formed aggregates (described below), no visible precipitate was observed, which did not prevent the CD study.<sup>34,35</sup> On the other hand, the CD spectrum of IGG did not change to that of a  $\beta$ -sheet structure, and only decrease of the helicity was observed even after 7 days (Fig. 2A). Such an incomplete transition to  $\beta$ -sheet was observed in case of butanoyl- or hexanoyl-attached peptides in our previous study.<sup>35</sup> The peptide lacking the N-terminal hydrophobic residue, GG, also did not show structural transition to  $\beta$ -sheet, and almost maintained the initial  $\alpha$ -helix structure during 7 days (Fig. 2B). Thus, it could be concluded that a hydrophobic amino acid at the N-termini is essential for the self-initiated structural transition of the peptide, but particular hydrophobic residues such as leucine, phenylalanine or tryptophan induce the  $\alpha$ -to- $\beta$  structural transition. These findings are consistent with our previous results<sup>34,35</sup> that the N-terminal hydrophobic domains such as Ad- or C8-group are essential for the structural transition and there is an optimum hydrophobicity to induce the transition.

To examine the peptides with further increased hydrophobicity at the N-termini, the peptides with one more residue added to the N-termini of LGG (ALGG, FLGG, ILGG, LLGG and WLGG) were prepared (Fig. 3). Among these peptides, only FLGG showed an accelerated structural transition (almost completed within 2 days) compared with LGG (Fig. 3A). The transitional properties of the other peptides (ALGG, ILGG, LLGG and WLGG) were not significantly altered compared with those of LGG (Fig. 3B). Although the addition of phenylalanine to the N-termini of LGG was effective for an acceleration of the transition, increase of the number of amino acids was not always effective. It is noteworthy that phenylalanine residues in the central hydrophobic region of Alzheimer's  $\beta$ -amyloid peptide have been proposed to play an important role in the fibril formation.<sup>38,39</sup>

The length of the spacer to connect the N-terminal hydrophobic residues with the core peptide portion was considered using the tryptophan-attached peptides, one of which was investigated as a peptide with a spectroscopic probe (described below). The peptides with one-glycine spacer, WG and WLG, were examined (Fig. 4). The  $\alpha$ -to- $\beta$  structural transition of WG was slightly retarded compared with that of WGG. The conformational change of WLG was much slow compared with that of WLGG. Furthermore, WLG did not show complete structural transition to  $\beta$ -sheet even after 7 days, although WLGG did within 4 days. These results revealed that the two-glycine spacer was more appropriate for induction of the structural transition than the one-glycine spacer. There may exist proper

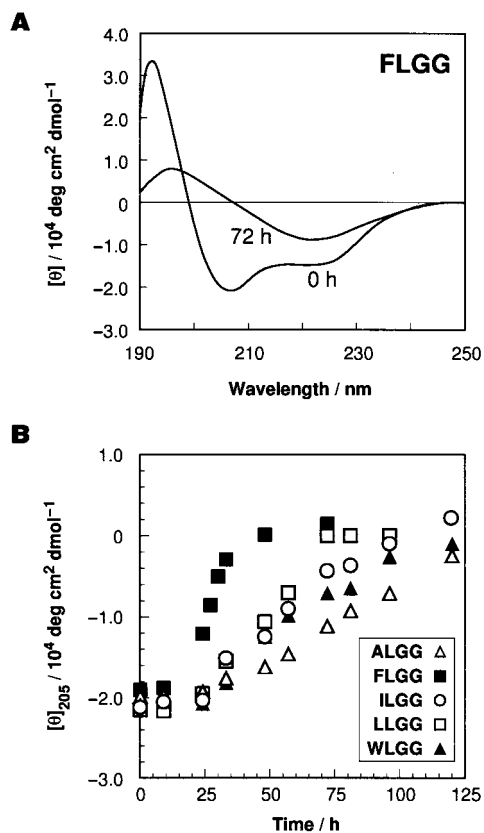


**Figure 3.** CD studies of the peptides with two hydrophobic residues at N-termini. (A) Time-dependent CD spectral changes of FLGG. (B) Time courses of structural transitions of the peptides monitored by the molar ellipticity at 205 nm. [Peptide]=12–13  $\mu\text{M}$  in 20 mM Tris–HCl buffer (pH 7.4)/2.5% TFE at 25°C.

length and flexibility of the N-terminal spacer so that the linked hydrophobic residues are exposed to the solvent.

The time courses of the  $\alpha$ -to- $\beta$  structural transition of the peptides were sigmoidal. This type of process is considered to be autocatalytic as suggested in the fibril formation of amyloidogenic proteins such as  $\beta$ -amyloid or prion proteins, and more generally, in crystallization of proteins or organic/inorganic compounds.<sup>8,34,35</sup> The autocatalytic transition

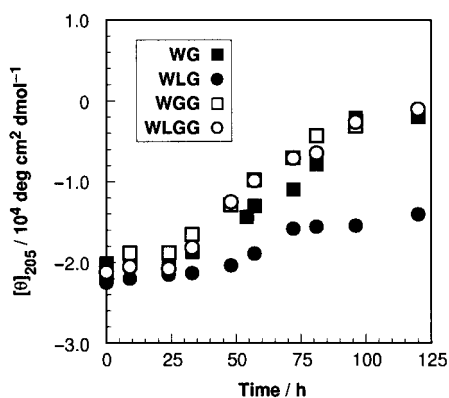


**Figure 4.** CD studies of the peptides with varied N-terminal spacers. Time courses of structural transitions of the peptides monitored by the molar ellipticity at 205 nm. [Peptide]=10–13  $\mu\text{M}$  in 20 mM Tris–HCl buffer (pH 7.4)/2.5% TFE at 25°C.

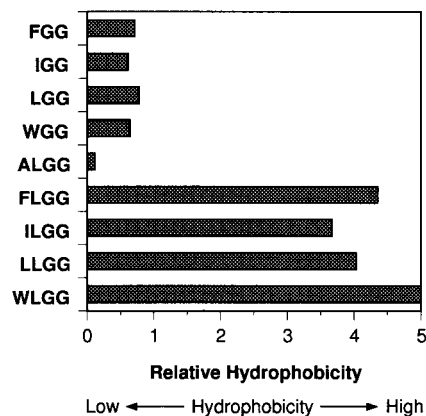


**Figure 5.** Relative hydrophobicity of the peptides determined by the retention times in reversed-phase HPLC, according to the method reported by Liu and Deber.<sup>40</sup> The most hydrophilic peptide GG and the most hydrophobic one WLGG are assigned with values of  $-5$  and  $+5$ , respectively.

process of this kind of peptide has been suggested by the fact that the  $\alpha$ -to- $\beta$  transition is accelerated by the addition of the preformed  $\beta$ -sheet peptide.<sup>34</sup>

#### Hydrophobicity of N-terminal residues of the peptides

In the previous study,<sup>35</sup> it was shown that only the peptides that had appropriate hydrophobic domains underwent the  $\alpha$ -to- $\beta$  structural transition. Thus, a hydrophobicity scale for this series was estimated using reversed-phase HPLC, as reported by Liu and Deber.<sup>40</sup> An HPLC-based scale serves to define the overall hydrophobicity of a peptide. Since all peptides have an identical chemical structure except for the N-terminal domain, their retention times would reflect the difference in hydrophobicity of the N-terminal domain. The HPLC experiments were carried out using a C18 column and the retention time data were converted to the relative hydrophobicity values<sup>40</sup> (Fig. 5). To compare only the hydrophobicity of the N-terminal residues, i.e. to eliminate a contribution of the glycine spacer, WG and WL were omitted from this analysis.

FLGG, which showed the highest transitional rate, had a higher hydrophobicity. However, it seems that the higher transitional rate of FLGG is not directly attributed to the higher hydrophobicity, since WLGG having a higher hydrophobicity than FLGG showed a slower transitional rate, and the peptides with two hydrophobic residues (ILGG, LLGG and WLGG) showed transitional rates similar to the peptides with single hydrophobic residue (FGG, LGG and WGG). Thus, the difference in the transitional rates is not explained only in terms of the hydrophobicity. Although N-terminal hydrophobic residues are essential for the induction of the structural transition, the increased hydrophobicity does not mean the increased transitional rate. Therefore, it appears that further addition of one or two hydrophobic residues is not always effective for acceleration of the transition. In addition, higher hydrophobicity at the N-termini may inhibit the transition, as shown in the previous study.<sup>35</sup>

In the course of our investigations,<sup>34,35</sup> we have proposed that a role of the N-terminal hydrophobic domain in the

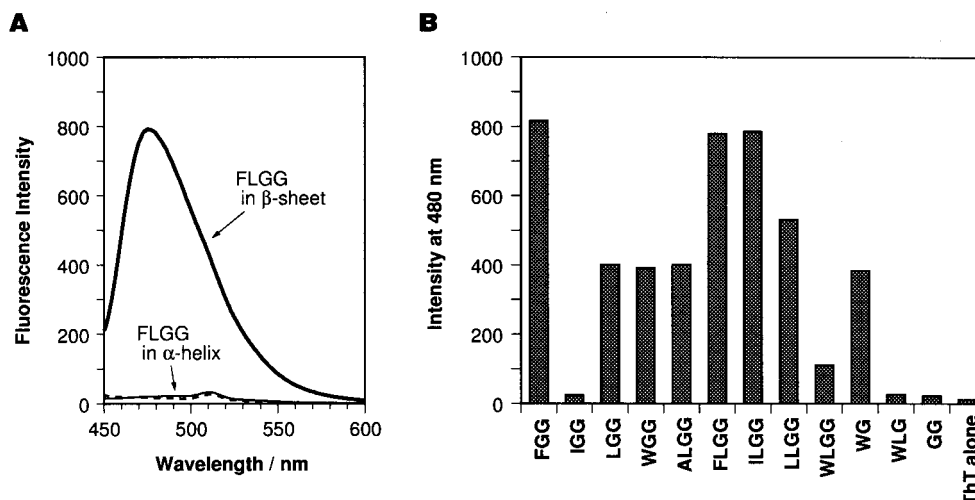


**Figure 6.** Thioflavin T (ThT) binding analysis of the peptides. (A) Fluorescence spectra of ThT in the presence of FLGG in  $\alpha$ -helix (thin line) or in  $\beta$ -sheet (bold line) and in the absence of the peptide (dashed line). (B) Fluorescence intensity of ThT at 480 nm in the presence of the peptides after the transitions. The peptides were incubated until they accomplished the transitions, and then ThT was added. [Peptide]=10–14  $\mu$ M and [ThT]=6  $\mu$ M in 20 mM Tris–HCl buffer (pH 7.4)/2.5% TFE at 25°C.  $\lambda_{\text{ex}}$ =435 nm.

process of the structural transition is the induction of intermolecular association of the  $\alpha$ -helical peptide by the hydrophobic interaction. Then, by the newly generated intermolecular interaction, the peptide transforms to a  $\beta$ -sheet structure. However, the N-terminal residues might also affect the stability of the assembled  $\beta$ -sheet structure, which would give rise to the difference in rates or completeness of the transitions. Therefore, an ability to form a fibrillar structure was examined as shown in the next section. Indeed, a self-assembling ability of the peptides in  $\beta$ -sheet to form the fibrillar structure was dependent on the residues attached to the N-termini (described below).

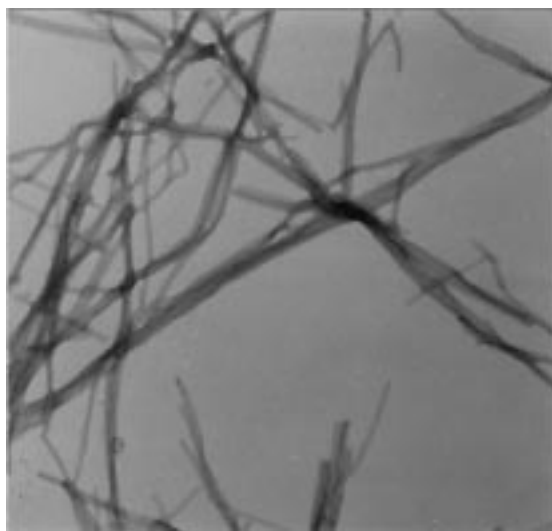


**Figure 7.** Electron micrograph of FLGG after the structural transition to  $\beta$ -sheet. The peptide was incubated until it accomplished the transition to  $\beta$ -sheet (3 days), and then negatively stained. Magnification, 50,000 $\times$ ; scale bar, 200 nm.

### Amyloid fibril formation of the peptides

The amyloid formation was examined employing an amyloid-specific dye-binding analysis (Fig. 6). It is known that a fluorescent dye, thioflavin T (ThT), associates with amyloid fibrils and the binding gives rise to a significant enhancement in fluorescence according to the amount of amyloid.<sup>34,41,42</sup> All peptides in  $\alpha$ -helix (shortly after dilution in the buffer from TFE) did not affect ThT fluorescence. The emission spectra of ThT in the presence of FLGG in  $\alpha$ -helix or  $\beta$ -sheet conformation are shown in Fig. 6A, as representative spectra of free and amyloid-bound ThT. In the presence of the peptides (except for IGG, WLG and GG) which accomplished the transition to  $\beta$ -sheet, ThT showed a new excitation maximum at  $\sim$ 435 nm and an enormously enhanced fluorescence emission at  $\sim$ 480 nm (Fig. 6B), which was a characteristic spectrum for ThT bound to amyloid fibrils. On the contrary, in the presence of the peptides which did not show complete transition to  $\beta$ -sheet, IGG, WLG and GG, the dye showed little enhancement in the fluorescence (Fig. 6B), suggesting the lack of an ability to form amyloid fibrils. The ThT-binding analysis suggested that the peptides except for IGG, WLG and GG had the ability to form amyloid fibrils. The ability, however, appeared to vary depending on the N-terminal residues. The fluorescence intensities of ThT in the presence of these peptides, which would reflect the amount of amyloid fibrils, were largely varied. These results imply that the N-terminal hydrophobic residues affect a well-organized assembly of the  $\beta$ -sheet into fibrils ( $\beta$ -sheet packing), as well as induction of the intermolecular association to initiate the structural transition.

A direct observation of the amyloid fibrils was also carried out by transmission electron microscopy. It was shown that the peptides which were expected to be amyloidogenic by the ThT-binding analysis indeed formed a fibrillar structure (Fig. 7). The fibrils had a morphology similar to that of naturally occurring amyloidogenic proteins such as  $\beta$ -amyloid or prion proteins.<sup>43,44</sup>

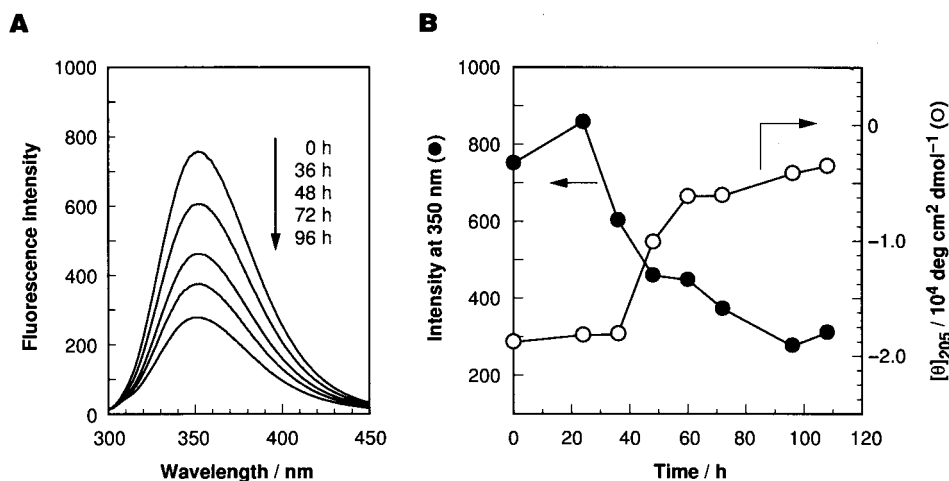


**Figure 8.** (A) Time-dependent fluorescence spectral changes of WGG. (B) Time courses of the fluorescence intensity at 350 nm and the molar ellipticity at 205 nm of WGG. [WGG]=13  $\mu$ M in 20 mM Tris–HCl buffer (pH 7.4)/2.5% TFE at 25°C.  $\lambda_{ex}$ =280 nm.

### Fluorescence spectroscopic study of the tryptophan-peptide

Fluorescence spectroscopic measurements were carried out for the tryptophan-containing peptide, which would provide information concerning the environment of tryptophan indole side chain.<sup>45</sup> The fluorescence spectra of WGG, which showed the  $\alpha$ -to- $\beta$  structural transition within 4 days, were measured (Fig. 8). The fluorescence emission maximum of WGG in the aqueous solution was 350 nm (Fig. 8A), suggesting the indole side chain was exposed to the solvent.<sup>45</sup> The time-dependent decrease in the fluorescence was observed, which was coincident with the CD spectral changes indicating the secondary structural transition (Fig. 8B). Although the aggregation of the peptide occurs during the  $\alpha$ -to- $\beta$  structural transition,<sup>34</sup> it is likely that the significant decrease in the fluorescence intensity is not due to the precipitation of the peptide, since the time-dependent changes of UV spectra were not large. Therefore, it could be considered that the decrease of the fluorescence intensity would be due to that the indole rings make clusters by aggregation and/or are buried in the assembled polypeptide chains, which occur during the  $\alpha$ -to- $\beta$  transition. The aggregation of the indole ring was also suggested by the result that the UV spectra were broadened during the  $\alpha$ -to- $\beta$  transition (data not shown).

CD spectra of the tryptophan in WGG at the near-UV region were measured. The asymmetric environments of the tryptophan side chain were expected to be changed during the  $\alpha$ -to- $\beta$  transition. However, the near-UV CD spectra of WGG before and after the transition were essentially identical (data not shown), suggesting little difference in the asymmetric environments of the tryptophan side chain. It is also expected that the mobility of tryptophan side chain in the aggregated  $\beta$ -sheet structure is more restricted than that in the  $\alpha$ -helix structure. Such further detailed information can be provided by a time-resolved fluorescence measurement.<sup>45</sup> Although the fluorescence and other spectroscopic data presented here are not sufficient to interpret the environments of tryptophan side chain, it is shown that the fluorescent amino acid is applicable as a spectroscopic

probe to follow the  $\alpha$ -to- $\beta$  transition, and as an inducer of the fibril formation by the hydrophobic character.

### Conclusion

In this paper, we present the design and synthesis of peptides undergoing a self-initiated structural transition from  $\alpha$ -helix to  $\beta$ -sheet and self-assembly into amyloid fibrils. We have succeeded in designing peptides composed of only standard amino acids retaining the transitional and fibril-forming abilities, whereas our previously reported peptides possessing these abilities contained non-amino acid moieties.<sup>34,35</sup> The peptides having hydrophobic amino acids in place of the Ad-group or the long acyl chains undergo the  $\alpha$ -to- $\beta$  structural transition, even though the transition takes a few days, which is much slower than that of Ad- or C8-attached peptides ( $\sim$ 4 h).<sup>34,35</sup> Some hydrophobic amino acids at the N-termini are appropriate to induce the  $\alpha$ -to- $\beta$  structural transition. Furthermore, the ability of self-assembly into fibrillar structure depends on the species of the hydrophobic residues attached to the N-termini.

Simplified model peptides like those presented here would lead to a better understanding of the process by which conformational alternation and aggregation of proteins occur, which will potentially lead to a model system for clarifying and controlling off-pathway aggregation of naturally occurring proteins. Moreover, since the amyloid fibril is a supramolecule with a highly ordered quaternary structure, the results demonstrated here will provide insights into studies on a structural basis of well-organized and self-assembling peptides applicable to novel nanoscale materials.<sup>23,24</sup>

### Experimental

#### Peptide synthesis

Peptides were synthesized by the solid phase method using

standard Fmoc chemistry.<sup>37</sup> The peptides were assembled on Rink amide resin, which provided C-terminal peptide amide on cleavage.<sup>46</sup> Fmoc-Ala-OH, Fmoc-Cys(Trt)-OH, Fmoc-Gln(Trt)-OH, Fmoc-Glu(OtBu)-OH, Fmoc-Gly-OH, Fmoc-Ile-OH, Fmoc-Leu-OH, Fmoc-Lys(Boc)-OH, Fmoc-Phe-OH, Fmoc-Trp-OH (*t*Bu, *tert*-butyl; Trt, trityl; Boc, *tert*-butyloxycarbonyl) were used. Couplings of Fmoc-protected amino acid were carried out using 2-(1*H*-benzotriazole-1-yl)-1,1,3,3-tetramethyluronium hexafluorophosphate (HBTU) and *N*-hydroxybenzotriazole (HOBT) in *N*-methylpyrrolidone (NMP), and Fmoc group was removed in 20% piperidine/NMP. The N-terminus was acetylated by treatment of acetic anhydride in NMP. Cleavage of the peptide from the resin and deprotection of all side chain protecting groups were carried out by stirring the resin in trifluoroacetic acid (TFA, 10 mL) in the presence of *m*-cresol (0.25 mL), thioanisole (0.75 mL) and ethanedithiol (0.75 mL) for 1 h at room temperature. The solution was filtered to remove the resin and the filtrate was concentrated, and then cold diethyl ether was added to precipitate the peptide. The crude peptides except for Trp-containing peptides were stirred in 10% dimethylsulfoxide (DMSO)/TFA for 2 h at room temperature to form the intermolecular disulfide linkage.<sup>47</sup> Trp-containing peptides were stirred in 50% DMSO/1 M HCl for 1–2 days to form the disulfide linkage.<sup>48</sup> The peptides were purified by reversed-phase HPLC on C18 or C4 columns (10×250 mm) using a linear gradient of acetonitrile/0.1% TFA to give a high purity on an analytical C18 column (4.6×150 mm). The peptides were identified by MALDI-TOFMS and amino acid analysis. MALDI-TOFMS were performed on a Shimadzu KOMPACT MALDI III mass spectrometer. MALDI-TOFMS found [M+H]<sup>+</sup> (calcd [M+H]<sup>+</sup>); FGG, 4088.8 (4089.8); IGG, 4022.4 (4021.8); LGG, 4022.1 (4021.8); WGG, 4167.9 (4167.9); GG, 3795.4 (3795.5); ALGG, 4163.1 (4163.9); FLGG, 4315.8 (4316.1); ILGG, 4247.6 (4248.1); LLGG, 4247.4 (4248.1); WLGG, 4394.1 (4394.2); WG, 4054.0 (4053.7); WLG, 4278.4 (4279.1). Amino acid analyses also gave satisfactory results.

### Circular dichroism spectroscopy

Stock solutions of the peptides were prepared in TFE (~0.5 mM peptide). The TFE solution was diluted in 20 mM Tris–HCl buffer (pH 7.4), final concentrations of the peptides were 10–14 μM and TFE content was 2.5%, and CD spectra were recorded immediately. After the dilution to the buffer from TFE, the solutions were incubated at 25°C and CD measurements were carried out at intervals of several hours. The concentration of each peptide solution was determined by the quantitative amino acid analysis. CD measurements were performed on a Jasco J-720WI spectropolarimeter equipped with a thermo-regulator using a quartz cell with 1.0 mm pathlength. Spectra were recorded in terms of mean residue ellipticity ([θ], in deg cm<sup>2</sup> dmol<sup>-1</sup>).

### Determination of hydrophobicity

HPLC-derived hydrophobicity was obtained by the retention time of each peptide on a C18 reversed-phase column (4.6×150 mm). Each peptide dissolved in TFE was injected into the column and eluted at a flow rate of 1.0 mL/min using a linear gradient of 30–70% acetonitrile/0.1% TFA

over 40 min at 40°C. The retention times of the peptides were converted to a relative hydrophathy index (*H*) by the following equation:

$$H = 10 \times \Delta t_{X-GG} / \Delta t_{WLGG-GG} - 5.00$$

where  $\Delta t_{X-GG}$  is the retention time difference between a peptide and the most hydrophilic peptide GG, and  $\Delta t_{WLGG-GG}$  is the retention time difference between the most hydrophobic peptide WLGG and GG.<sup>40</sup>

### Fluorescence and UV spectroscopies

Peptide solution was prepared and incubated as described in the CD measurements (10–14 μM peptide in 20 mM Tris–HCl buffer (pH 7.4) with 2.5% TFE at 25°C). For ThT-binding analysis, 10 μL of the ThT solution (240 μM in water) was added to 390 μL of the peptide solution (the final concentrations of ThT and the peptide were 6 and 10–14 μM, respectively), and then fluorescence emission spectra were recorded immediately at an excitation wavelength of 435 nm.<sup>34,41,42</sup> For the measurements of the tryptophan-peptide, the indole side chain was excited at 280 nm. Fluorescence spectra were recorded on a Hitachi F-2500 fluorescence spectrophotometer using a 5×5 mm quartz cell at 25°C. UV spectra were recorded on a Shimadzu BioSpec-1600 UV–VIS spectrophotometer using a quartz cell with 10 mm pathlength.

### Transmission electron microscopy

The peptide solution was prepared by the method same as the CD measurement. The sample was absorbed to a carbon-coated copper grid (200 mesh) by floating the grid on a drop of the peptide solution for 30 s. The excess solution was removed by filter paper blotting and the grid was washed by floating on a drop of water for 10 s and then the water was removed. The sample on the grid was then negatively stained with a 2% (w/v) aqueous phosphotungstic acid solution for 30 s and the excess staining solution was removed. After drying, the samples were visualized with a Hitachi H-7500 electron microscope operating at 100 kV.

### References

1. Fink, A. L. *Fold. Des.* **1998**, *3*, R9–R23.
2. Dobson, C. M. *Trends Biochem. Sci.* **1999**, *24*, 329–332.
3. Kelly, J. W. *Curr. Opin. Struct. Biol.* **1998**, *8*, 101–106.
4. Booth, D. R.; Sunde, M.; Bellotti, V.; Robinson, C. V.; Hutchinson, W. L.; Fraser, P. E.; Hawkins, P. N.; Dobson, C. M.; Radford, S. E.; Blanke, C. C. F.; Pepys, M. B. *Nature* **1997**, *385*, 787–793.
5. Mihara, H.; Takahashi, Y. *Curr. Opin. Struct. Biol.* **1997**, *7*, 501–508.
6. Mihara, H.; Takahashi, Y.; Ueno, A. *Biopolymers* **1998**, *47*, 83–92.
7. Kelly, J. W.; Lansbury Jr, P. T. *Amyloid: Int. J. Exp. Clin. Invest.* **1994**, *1*, 186–205.
8. Harper, J. D.; Lansbury Jr., P. T. *Annu. Rev. Biochem.* **1997**, *66*, 385–407.
9. Selkoe, D. J. *J. Biol. Chem.* **1996**, *271*, 18295–18298.
10. Coles, M.; Bicknell, W.; Watson, A. A.; Fairlie, D. P.; Craik, D. J. *Biochemistry* **1998**, *37*, 11064–11077.

11. Shao, H.; Jao, S.; Ma, K.; Zagorski, M. G. *J. Mol. Biol.* **1999**, *285*, 755–773.
12. Prusiner, S. B. *Science* **1997**, *278*, 245–251.
13. Harrison, P. M.; Bamborough, P.; Daggett, V.; Prusiner, S. B.; Cohen, F. E. *Curr. Opin. Struct. Biol.* **1997**, *7*, 53–59.
14. Riek, R.; Hornemann, S.; Wider, G.; Glockshuber, R.; Wüthrich, K. *FEBS Lett.* **1997**, *413*, 282–288.
15. Guijarro, J. I.; Sunde, M.; Jones, J. A.; Campbell, I. D.; Dobson, C. M. *Proc. Natl. Acad. Sci. USA* **1998**, *95*, 4224–4228.
16. Chiti, F.; Webster, P.; Taddei, N.; Clark, A.; Stefani, M.; Ramponi, G.; Dobson, C. M. *Proc. Natl. Acad. Sci. USA* **1999**, *96*, 3590–3594.
17. DeGrado, W. F.; Summa, C. M.; Pavone, V.; Nistri, F.; Lombardi, A. *Annu. Rev. Biochem.* **1999**, *68*, 779–819.
18. Schneider, J. P.; Kelly, J. W. *Chem. Rev.* **1995**, *95*, 2169–2187.
19. Gellman, S. H. *Curr. Opin. Chem. Biol.* **1998**, *2*, 717–725.
20. Choo, D. W.; Schneider, J. P.; Graciani, N. R.; Kelly, J. W. *Macromolecules* **1996**, *29*, 355–366.
21. West, M. W.; Wang, W.; Patterson, J.; Mancias, J. D.; Beasley, J. R.; Hecht, M. H. *Proc. Natl. Acad. Sci. USA* **1999**, *96*, 11211–11216.
22. Lazo, N. D.; Downing, D. T. *Biochem. Biophys. Res. Commun.* **1997**, *235*, 675–679.
23. Aggeli, A.; Bell, M.; Boden, N.; Keen, J. N.; Knowles, P. F.; McLeish, T. C. B.; Pitkeathly, M.; Radford, S. E. *Nature* **1997**, *386*, 259–262.
24. Zhang, S.; Rich, A. *Proc. Natl. Acad. Sci. USA* **1997**, *94*, 23–28.
25. Minor Jr, D. L.; Kim, P. S. *Nature* **1996**, *380*, 730–734.
26. Dalal, S.; Balasubramanian, S.; Regan, L. *Nat. Struct. Biol.* **1997**, *4*, 548–552.
27. Cordes, M. H. J.; Walsh, N. P.; McKnight, C. J.; Sauer, R. T. *Science* **1999**, *284*, 325–327.
28. Mutter, M.; Hersperger, R. *Angew. Chem., Int. Ed. Engl.* **1990**, *29*, 185–187.
29. Ono, S.; Kameda, N.; Yoshimura, T.; Shimasaki, C.; Tsukuromichi, E.; Mihara, H.; Nishino, N. *Chem. Lett.* **1995**, 965–966.
30. Mutter, M.; Gassmann, R.; Buttkus, U.; Altmann, K.-H. *Angew. Chem., Int. Ed. Engl.* **1991**, *30*, 1514–1516.
31. Schenck, H. L.; Dado, G. P.; Gellman, S. H. *J. Am. Chem. Soc.* **1996**, *118*, 12487–12494.
32. Sakamoto, S.; Obataya, I.; Ueno, A.; Mihara, H. *Chem. Commun.* **1999**, 1111–1112.
33. Kuwata, K.; Hoshino, M.; Era, S.; Batt, C. A.; Goto, Y. *J. Mol. Biol.* **1998**, *283*, 731–739.
34. Takahashi, Y.; Ueno, A.; Mihara, H. *Chem. Eur. J.* **1998**, *4*, 2475–2484.
35. Takahashi, Y.; Ueno, A.; Mihara, H. *Bioorg. Med. Chem.* **1999**, *7*, 177–185.
36. Kohn, W. D.; Hodges, R. S. *Trends Biotechnol.* **1998**, *16*, 379–389.
37. Atherton, E.; Sheppard, R. C. *Solid Phase Peptide Synthesis: A Practical Approach*, IRL: Oxford, 1989.
38. Hilbich, C.; Kisters-Woike, B.; Reed, J.; Masters, C. L.; Beyreuther, K. *J. Mol. Biol.* **1992**, *228*, 460–473.
39. Esler, W. P.; Stimson, E. R.; Ghilardi, J. R.; Lu, Y.-A.; Felix, A. M.; Vinters, H. V.; Mantyh, P. W.; Maggio, J. E. *Biochemistry* **1996**, *35*, 13914–13921.
40. Liu, L.-P.; Deber, C. M. *Biopolymers* **1998**, *47*, 41–62.
41. LeVine III, H. *Protein Sci.* **1993**, *2*, 404–410.
42. Soto, C.; Sigurdsson, E. M.; Morelli, L.; Kumar, R. A.; Castaño, E. M.; Frangione, B. *Nat. Med.* **1998**, *4*, 822–826.
43. Wood, S. J.; Maleeff, B.; Hart, T.; Wetzel, R. *J. Mol. Biol.* **1996**, *256*, 870–877.
44. Nguyen, J. T.; Inouye, H.; Baldwin, M. A.; Fletterick, R. J.; Cohen, F. E.; Prusiner, S. B.; Kirschner, D. A. *J. Mol. Biol.* **1995**, *252*, 412–422.
45. Handel, T. M.; Williams, S. A.; Menyhard, D.; DeGrado, W. F. *J. Am. Chem. Soc.* **1993**, *115*, 4457–4460.
46. Rink, H. *Tetrahedron Lett.* **1987**, *28*, 3787–3790.
47. Otaka, A.; Koide, T.; Shide, A.; Fujii, N. *Tetrahedron Lett.* **1991**, *32*, 1223–1226.
48. Tamamura, H.; Otaka, A.; Nakamura, J.; Okubo, K.; Koide, T.; Ikeda, K.; Fujii, N. *Tetrahedron Lett.* **1993**, *34*, 4931–4934.